

On the characterization of crystallization and ice adhesion on smooth and rough surfaces using molecular dynamics

Cite as: Appl. Phys. Lett. **104**, 021603 (2014); <https://doi.org/10.1063/1.4862257>

Submitted: 14 September 2013 . Accepted: 02 January 2014 . Published Online: 16 January 2014

Jayant K. Singh, and Florian Müller-Plathe



View Online



Export Citation



CrossMark

ARTICLES YOU MAY BE INTERESTED IN

[Frost formation and ice adhesion on superhydrophobic surfaces](#)

Applied Physics Letters **97**, 234102 (2010); <https://doi.org/10.1063/1.3524513>

[Molecular simulations of heterogeneous ice nucleation. I. Controlling ice nucleation through surface hydrophilicity](#)

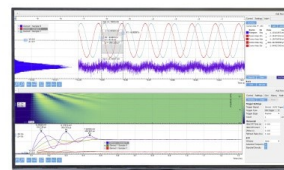
The Journal of Chemical Physics **142**, 184704 (2015); <https://doi.org/10.1063/1.4919714>

[A potential model for the study of ices and amorphous water: TIP4P/Ice](#)

The Journal of Chemical Physics **122**, 234511 (2005); <https://doi.org/10.1063/1.1931662>

Challenge us.

What are your needs for
periodic signal detection?



Zurich
Instruments

On the characterization of crystallization and ice adhesion on smooth and rough surfaces using molecular dynamics

Jayant K. Singh^{1,2,a)} and Florian Müller-Plathe¹

¹Eduard-Zintl-Institut für Anorganische und Physikalische Chemie, Technische Universität Darmstadt, Petersenstr. 20, D-64287 Darmstadt, Germany

²Department of Chemical Engineering, Indian Institute of Technology Kanpur, Kanpur 208016, India

(Received 14 September 2013; accepted 2 January 2014; published online 16 January 2014)

Coarse-grained molecular dynamics is utilized to quantify the behavior of a supercooled water drop on smooth and rough surfaces. Crystallization on rough surface is characterized based on wetting states. Freezing temperature and work of adhesion of water droplet are linearly associated with roughness parameters corresponding to the Cassie-Baxter and Wenzel states. The behavior is insensitive to different surface-fluid affinity. We show in general, for Wenzel states, work of adhesion is higher than that of Cassie-Baxter state for surfaces that have identical freezing temperatures. © 2014 AIP Publishing LLC. [<http://dx.doi.org/10.1063/1.4862257>]

Formation of ice on surfaces can adversely affect industrial processes and applications in daily life such as in power lines, aircraft, ships, and buildings.^{1,2} Thus, there have recently been efforts to design such ice-repellant surfaces, and many of them have been inspired by the successes in the design of super-hydrophobic surfaces.^{3–14} However, the influence of surface texture is less understood for de-icing application, and attempts have been made to find linear correlation between the equilibrium work of adhesion of ice and the wettability of the substrate by liquid water ($1 + \cos \theta$), where θ is the equilibrium (Young's) contact angle.^{15,16} Early attempts by Murase *et al.*¹⁷ resulted in a significant scatter in the data, leading to weak correlation of the above expression. However, Meuler *et al.*¹⁸ have recently confirmed the above correlation to hold between the work of ice adhesion (work to remove ice from the surface) and the receding contact angle of liquid water, for various surface coatings. They concluded that a reduction of the ice adhesion strength requires a surface on which water droplets exist in the Cassie-Baxter state (drop suspended on surface protrusions) before freezing occurs.

While some experiments indicate that superhydrophobic surface can minimize or eliminate ice formation, under some conditions,¹⁹ other experiments, for example of Jung *et al.*,²⁰ conclude that anti-icing design needs optimization of the competing influence of both freezing delay and liquid-

shedding ability, i.e., low adhesion. Recent work of Nosonovsky and Hejazi,²¹ based on the theoretical analysis of mechanical forces acting on a liquid droplet and ice, suggests that it depends on the size of the roughness whether or not a superhydrophobic surface is at the same time ice-phobic. This is in line with the prediction²² of a hard-sphere model that there is a optimal pit size on the surface for unrestrained growth of crystals. Furthermore, the lattice commensurability and incommensurability can affect crystal nucleation dramatically.²³ Moreover, the claim of Chen and co-workers that superhydrophobic surfaces cannot reduce ice adhesion²⁴ further corroborates other findings.

Hence, the apparent contradictions of experiments confuse the picture of the role of roughness for the design of anti-icing surfaces. In this Letter, we demonstrate, using molecular dynamics, that freezing temperature and work of adhesion of liquid water, can be directly correlated with parameters of nanoscale roughness, if dependence on the wetting state is allowed for. Furthermore, we demonstrate clearly that the crystallization behavior on the rough surface can be characterized based on the wetting state of the liquid drops, and we extend the validity of an earlier continuum equation^{25,26} to the *supercooled drop-surface* systems.

We use the coarse grain monatomic water model mW,²⁷ which consists of two-body, ϕ_2 , and three-body contributions, ϕ_3

$$\begin{aligned}
 U &= \sum_i \sum_{i>j} \phi_2(r_{ij}) + \sum_i \sum_{j \neq i} \sum_{k>j} \phi_3(r_{ij}, r_{ik}, \theta_{ijk}), \\
 \phi_2(r_{ij}) &= A\epsilon \left[B \left(\frac{\sigma}{r_{ij}} \right)^p - 1 \right] \exp\left(\frac{\sigma}{r_{ij} - a\sigma} \right), \\
 \phi_3(r_{ij}, r_{ik}, \theta_{ijk}) &= \lambda\epsilon [\cos \theta_{ijk} - \cos \theta_0]^2 \exp\left(\frac{\gamma\sigma}{r_{ij} - a\sigma} \right) \exp\left(\frac{\gamma\sigma}{r_{ik} - a\sigma} \right),
 \end{aligned} \tag{1}$$

^{a)}Electronic mail: jayantks@iitk.ac.in

where r_{ij} is the distance between particles i and j ; θ_{ijk} is the angle between the vectors joining i and j , and i and k . $A = 7.049556277$, $B = 0.6022245584$, $p = 4$, $\gamma = 1.2$, $a = 1.8$, $\theta_0 = 109.47^\circ$, $\sigma = 2.3925 \text{ \AA}$, $\varepsilon = 6.189 \text{ kcal/mol}$, and $\lambda = 23.15$.

A smooth surface is modeled using two atomistic graphene layers (bond length of 1.42 \AA , interlayer spacing of 3.54 \AA). Texture is designed on top of the two graphene base layers, by using pillars made out of additional graphite sheets. Pillar width and pillar gap are in the order of $10\text{--}20 \text{ \AA}$. Pillar heights are varied in the range of $10\text{--}20 \text{ \AA}$. Graphene atoms are kept immobile during the simulation. The contact angle is calculated by the procedure of Werder *et al.*²⁸

The interaction of a water molecule with surface atoms is modeled with the two-body part of Eq. (1); σ_{ws} is fixed at 3.2 \AA , and ε_{ws} is varied in the range of $0.05\text{--}0.15 \text{ kcal/mol}$.²⁹ The other parameters are identical to those of the water-water potential. A local bond orientational order parameter³⁰ is used for each atom i to identify the ice structure following the procedure of Li *et al.*³¹ LAMMPS³² is used with the velocity-Verlet algorithm and a time step of 10 fs to carry out all molecular dynamics simulations. The number of surface atoms ranges from $12\,000$ to $30\,000$ depending on the desired surface roughness. The surface is around $140 \text{ \AA} \times 140 \text{ \AA}$. Periodic boundary conditions are applied in all directions. The number of water molecules, N , is always $1\,963$. The system is initially equilibrated for 10 ns at 270 K (liquid) and 1 atm . A Nosé-Hoover thermostat and barostat (only in the z direction) are used to keep the temperature and pressure fixed, respectively.

We first simulated the nanodroplet without any surface at a cooling rate of 0.1 K/ns . The freezing temperature is found to be $194 \pm 2 \text{ K}$, in line with the prediction of Fletcher,³³ which states that freezing temperature reduces with decrease of the drop radius. Bulk mW freezes at $\sim 200 \text{ K}$.³⁴ The simulation with the surface is first cooled at 0.5 K/ns at 1 atm to $T = 220 \text{ K}$. Then the system is further cooled at constant volume to $T = 170 \text{ K}$. At 170 K , an additional 200 ns run is conducted. The spatial distribution of the crystalline phases seen here is similar to that observed in an earlier work.³¹

Crystallization of a water nanodroplet on the surface proceeds in three steps, as shown in Fig. 1(a). In the first stage, the number of ice-like particles grows sufficiently to form a critical nucleus ($\sim 40\text{--}60$). This is followed by the second stage, a sudden phase transition, in which the number of ice-like molecules explodes. This is more evident in Fig. 1(b), which shows continuous decrease in energy with reducing temperature until the phase transition. The third stage is slow incorporation of remaining free particles into the ice phase. Although the final number of ice-like particles does not depend on the water-surface interaction ε_{ws} , the growth of the ice nuclei leading to critical size for the transition is affected by it. With increasing attraction, the phase transition occurs at a higher temperature, i.e., higher hydrophilicity speeds up crystallization leading to a higher freezing temperature. The corresponding potential energy of the system (Fig. 1(b)) shows a visible decrease associated not only with the fast crystal growth stage (2), but also the slow phases of nucleation (1) and crystal healing (3).

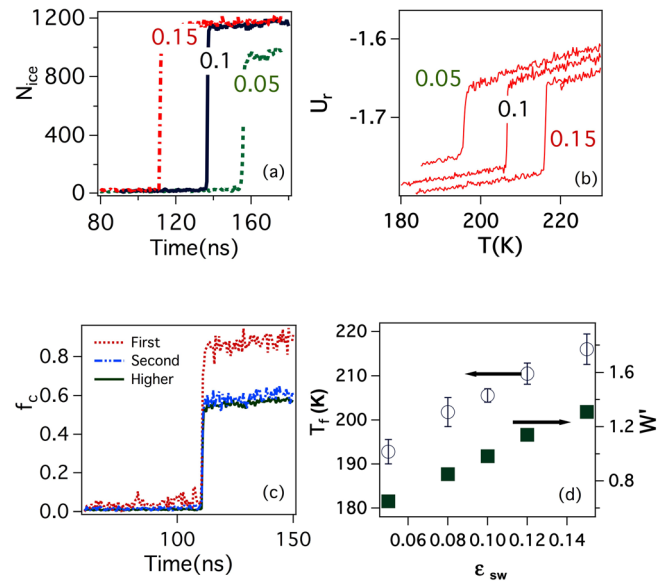


FIG. 1. (a) Number of ice-like molecules as a function temperature for different water-surface interaction strengths ε_{ws} (kcal/mol). (b) Reduced potential energy of the drop $U_r = (U/\varepsilon N)$. (c) Ice fraction in the first, second, and higher layers for a smooth surface with $\varepsilon_{ws} = 0.1 \text{ kcal/mol}$. (d) Freezing temperature (open circles, the error bars are the standard deviations between 4–6 independent simulations), and reduced work of adhesion W' at 270 K (filled squares) of water droplet on smooth surface as a function of water-surface affinity.

One long-standing question is the spatial preference of nucleation events. Do they start from the substrate surface or from the bulk? Heterogeneous nucleation has been investigated using simple models.^{35,36} For example, Xu *et al.*³⁶ showed that the duration of a metastable fluid state can be reduced or eliminated by patterned surfaces via a reduction in the free-energy barrier. This is in line with Auer and Frenkel,³⁷ who state that a commensurate substrate can lead to a negligible ($\sim k_B T$) nucleation barrier. Recently, molecular dynamics has shown that tetrahedral fluids, based on the Stillinger-Weber potential for silicon and germanium, crystallize faster by several orders³⁸ in the presence of a free surface. This model is similar to the mW model used in this work; hence, we expect similar behavior. Fig. 1(c) shows the ice-like fraction for first, second, and higher layers, distinguished based on the density profile, with time. The first layer has the largest ice content at all temperatures; it crystallizes to 9%, whereas the remaining layers, including the second, are still 40% liquid like at 190 K (corresponding to 160 ns run length). This confirms that crystallization preferentially occurs at the surface, which is further evident from the ice profile (see supplementary material for Figure S1).⁴¹ This is in line with the earlier observations for hard-sphere fluids on patterned substrate.^{35,37}

We determine the freezing temperature as the temperature at which sharp drop in the energy and sharp jump in the fraction of ice particles are seen. To obtain an estimate, 4–6 independent simulations are performed. The freezing temperature increases linearly with the surface-water interaction strength ε_{sw} as shown in Fig. 1(d). We also analyze the contact angle of the drop in the liquid state (270 K) and estimate from it the work of adhesion of liquid drop (per unit area) as $W_{adh} = \gamma_{lv}(1 + \cos\theta)$.¹⁶ The work of adhesion is

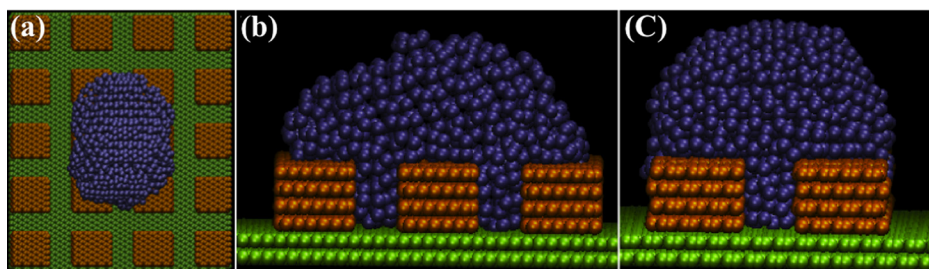


FIG. 2. A snap shot of the super cooled water in the Wenzel state at 170 K for $\phi = 0.9$ and $\epsilon_{sw} = 0.15$. Panel a is the top view, and b and c are the side views.

also defined as $W_{adh} \sim \gamma_{surf} + \gamma_l - \gamma_i$,¹⁶ where subscripts *surf*, *l*, and *i* stand for substrate, liquid, and solid-liquid interface, respectively. It follows that, wettability or reduced work of adhesion, $W' = W_{adh}/\gamma_{lv} = (1 + \cos \theta) \approx \frac{-\gamma_i + C}{\gamma_{lv}}$. Fig. 1(d) also presents the W' (a larger number means stronger adhesion or more wettable), with ϵ_{sw} . The dependence is linear for W' , and thus it also correlates well with the freezing temperature. The interfacial tension thus becomes more negative with ϵ_{sw} , indicative of stronger adhesion leading to higher freezing temperature. To summarize, an atomically smooth surface clearly shows an easier onset of crystallization with higher hydrophilicity. The data, however, are not in agreement with recent experiments done on “smooth” surfaces, where the hydrophilic surface is found to reduce the crystallization rate.³⁹ We attribute the difference to the residual molecular roughness on the hydrophilic (which was coated) and hydrophobic surfaces, used in the experiments.

We now address the crystallization behavior on rough surfaces (see supplementary material for Figure S2).⁴¹ We define the following parameters: fractional projected area, $\alpha = (\text{projected area of pillars in the unit cell})/(\text{unit cell cross-section area})$, and the roughness factor $r = (\text{actual wettable area})/(\text{unit cell-cross sectional area})$, which are commonly used to describe Cassie-Baxter (water drop suspended on surface protrusions) and Wenzel (water entering the spaces between protrusions) states, respectively. Fig. 2 presents a typical snapshot of the water droplet in the

Wenzel state. Corresponding crystallization states at different run time are shown in Fig. 3. The freezing temperature is calculated akin to that for the smooth surface, which for the case as in Fig. 3 is 198 ± 2 K corresponding to ~ 143.5 ns. Similar estimates have been evaluated for other cases as studied in this work (see supplementary material for Tables S1, S2, Figures S3–S6).⁴¹ Fig. 4(a) summarizes the freezing temperature for $\epsilon_{sw} = 0.1$ kcal/mol as a function of fractional projected area, α .

While the data do not suggest any explicit correlation, the freezing temperature, nevertheless, increases with increasing fraction of the projected area, α . The overall scatter in the data seen in Fig. 4(a) mainly is due to the presence of Wenzel states, as identified by the density and energy profiles (see supplementary material for Figure S7).⁴¹ Fig. 4(b) presents the freezing temperature against r , which, as expected, increases with decreasing fractional rough area, and approaches that of the smooth surface. However, the data are scattered and do not yield a good correlation. This is due to the presence of Cassie-Baxter states in the data (see supplementary material for Figure S7).⁴¹ It is evident that the freezing behavior cannot be clearly correlated to surface features if wetting states are ignored.

In order to find a clearer interpretation, we resort to the work on liquid near rough surfaces of Leroy and Müller-Plathe,^{25,26} who showed that down to molecular dimensions the solid-liquid interfacial tension, γ_{sl} , is directly correlated

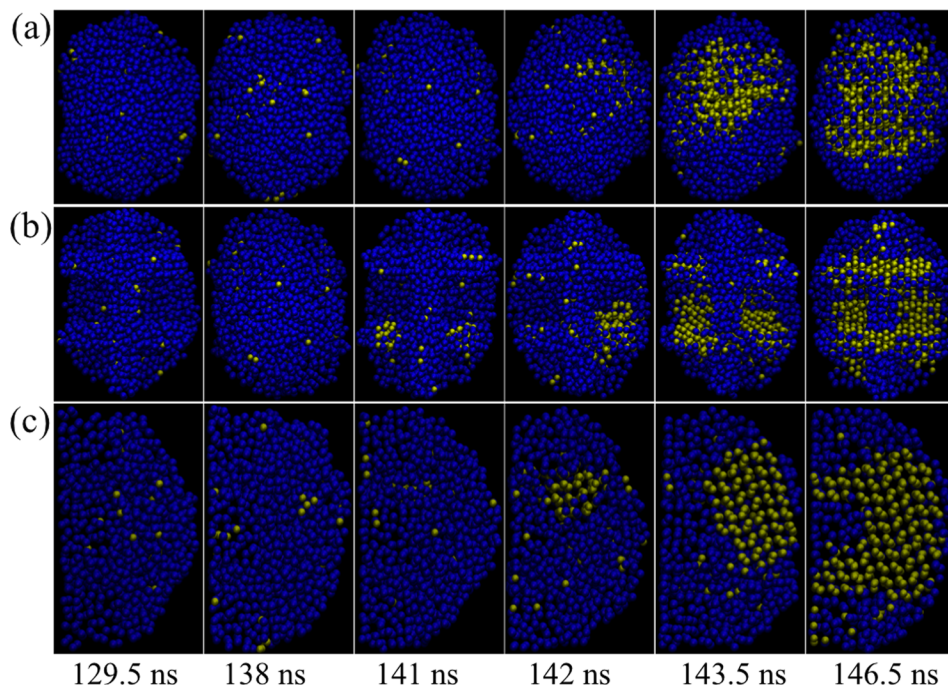


FIG. 3. Snapshots of crystallization of water drop in the Wenzel state at $\phi = 0.9$ and $\epsilon_{sw} = 0.15$, with simulation run time. Row a is the top view, b is the side view, and c is the cross-sectional view. The molecules belonging to the ice cores are shown in yellow.

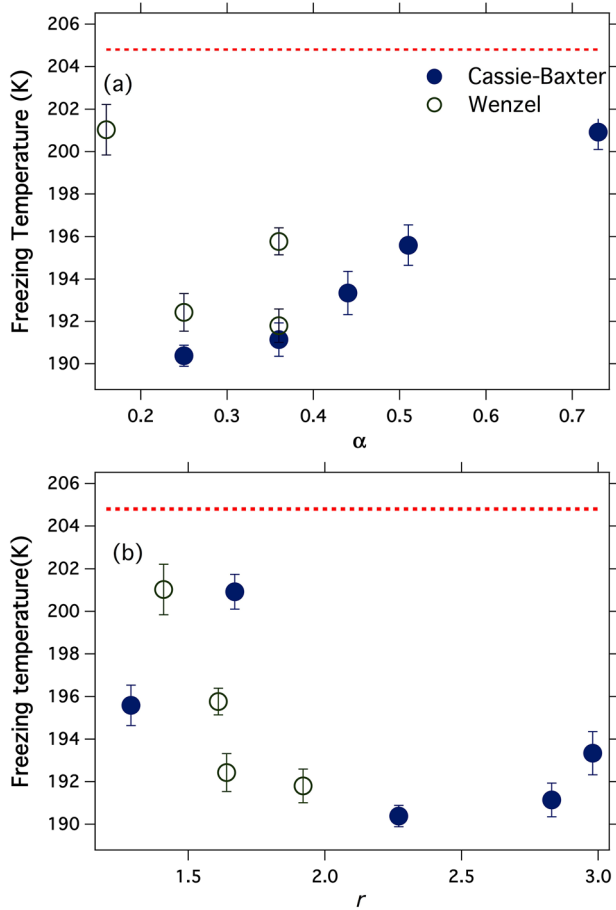


FIG. 4. (a): Freezing temperature as a function of roughness parameter α associated with the Cassie-Baxter case; (b) freezing temperature as a function of roughness parameter r corresponding to the Wenzel case. The surface affinity is fixed at $\epsilon_{sw} = 0.1$ kcal/mol. The dashed line represents the freezing temperature for the smooth surface. Each symbol represents a unique surface, where either Wenzel or Cassie-Baxter state is observed.

with different roughness parameters for the two wetting states. For the Cassie-Baxter-states, it is proportional to the fractional projected area: $\gamma_{sl} \propto \alpha$.²⁵ In contrast, for the Wenzel states, the solid-liquid interfacial tension of a groove system is the weighted average of horizontal and vertical regions of the groove:²⁶ $\gamma_{sl,groove} = \gamma_{sl,groove,H} + \phi \gamma_{sl,groove,V}$, with the heterogeneity factor $\phi = (\text{area of the vertical surface}) / (\text{unit cell cross-sectional area})$. Taking into account the limiting values of the solid-liquid tension of the horizontal and vertical sections, the surface tension of the groove system, $\gamma_{sl} \propto \phi$. Since the work of adhesion is directly proportional to the interfacial tension, W' should be linearly related to α and ϕ for the two wetting states, which is indeed observed in Figs. 5(a) and 5(b). The data, which were scattered in Figs. 4(a) and 4(b), are now linear in the roughness parameters associated with Cassie-Baxter and Wenzel states. The relation between freezing temperature and W' , established above for flat surfaces, is seen to hold also for structured surfaces and different surface-fluid affinities. Figs. 5(a) and 5(b) also contain the reduced total energy of the system, which is found to be linear in the surface-fluid affinity. In case of Cassie states, increasing α turns the surface smoother, which due to higher contact with the surface, lead to a linearly increase of W' and T_f with α (and a decrease of the

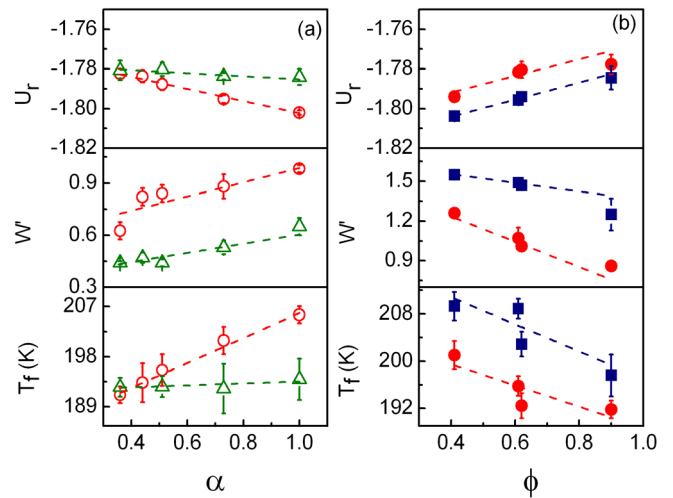


FIG. 5. Freezing temperature, reduced work of adhesion, W' at 270 K, and potential energy of the drop at 190 K vs. roughness parameters, α and ϕ (a) Cassie-Baxter states, (b) Wenzel states. Symbols circle, triangle and square represent surface-fluid affinities (in kcal/mol): 0.1, 0.05, and 0.15, respectively.

potential energy). In contrast, the effect of the base layer diminishes with increasing ϕ leading to an increase of the drop energy and a decrease in the corresponding work of adhesion. This in effect reduces the freezing temperature of Wenzel drop with increasing ϕ . The reduced work of adhesion follows the same trend as the freezing temperature (see supplementary material for Tables S1 and S2).⁴¹

Do the surfaces with a similar freezing temperature also have a similar work of adhesion? Fig. 6 summarizes the results for different wetting states. It turns out that the freezing temperature is almost linear in the work of adhesion, for the two wetting states treated separately. Simulation points deviating from the straight line are mainly due to departure from the ideal Cassie-Baxter or Wenzel state. It is clear from Fig. 6 that two surfaces having similar freezing temperature can have drastically different work of adhesion, if the wetting states are different. Wenzel states invariably have higher work of adhesion compared to Cassie-Baxter states. This

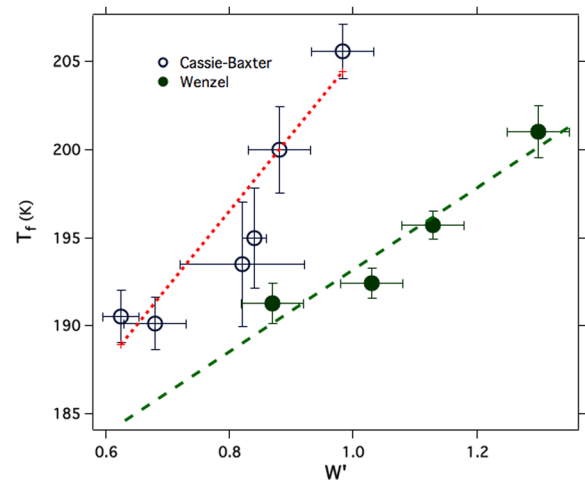


FIG. 6. Freezing temperature against reduced work of adhesion W' for rough surfaces with different wetting states and $\epsilon_{sw} = 0.1$ kcal/mol. W' is averaged over 4 simulations at 270 K. Error bar represents standard deviation based on 4-6 simulations.

indeed supports various experimental observations,^{24,40} where high ice adhesion has been observed mainly because of a transition from the Cassie-Baxter state to the Wenzel state during the cooling process, before crystallization.

In summary, using molecular dynamics simulations, we demonstrate a linear relation of reduced work of adhesion and freezing temperature with corresponding roughness parameters for the Cassie-Baxter and Wenzel states. Further, this work emphasizes the importance of the Cassie-Baxter state, as a design goal for ice-phobic surfaces.¹⁸

J.K.S. wish to thank Alexander von Humboldt Foundation for financial support. J.K.S. also thanks Dr. Frédéric Leroy for stimulating discussions. This work was partially supported by the Department of Science and Technology, India.

- ¹V. A. Croutch and R. A. Hartley, *J. Coat. Technol.* **64**, 41 (1992).
- ²L. L. Cao, A. K. Jones, V. K. Sikka, J. Z. Wu, and D. Gao, *Langmuir* **25**, 12444 (2009).
- ³W. Barthlott and C. Neinhuis, *Planta* **202**, 1 (1997).
- ⁴C. Ran, G. Ding, W. Liu, Y. Deng, and W. Hou, *Langmuir* **24**, 9952 (2008).
- ⁵Z. Yoshimitsu, A. Nakajima, T. Watanabe, and K. Hashimoto, *Langmuir* **18**, 5818 (2002).
- ⁶D. M. Spori, T. Drobek, S. Zürcher, M. Ochsner, C. Sprecher, A. Mühlebach, and N. D. Spencer, *Langmuir* **24**, 5411 (2008).
- ⁷N. J. Shirtcliffe, G. McHale, M. I. Newton, and C. C. Perry, *Langmuir* **21**, 937 (2005).
- ⁸H. Modaressi and G. Garnier, *Langmuir* **18**, 642 (2002).
- ⁹F. Heslot, A. M. Cazabat, P. Levinson, and N. Fraysse, *Phys. Rev. Lett.* **65**, 599 (1990).
- ¹⁰G. O. Berim and E. Ruckenstein, *J. Chem. Phys.* **130**, 184712 (2009).
- ¹¹J. Yaneva, A. Milchev, and K. Binder, *J. Chem. Phys.* **121**, 12632 (2004).
- ¹²M. Lundgren, N. L. Allan, and T. Cosgrove, *Langmuir* **23**, 1187 (2007).
- ¹³G. S. Grest, D. R. Heine, and E. B. Webb, *Langmuir* **22**, 4745 (2006).
- ¹⁴J. T. Hirvi and T. A. Pakkanen, *J. Chem. Phys.* **125**, 144712 (2006).
- ¹⁵T. Young, *Philos. Trans. R. Soc. London* **95**, 65 (1805).
- ¹⁶J. N. Israelachvili, *Intermolecular and Surface Forces* (Academic press, London, 1992).
- ¹⁷H. Murase, K. Nanishi, H. Kogure, T. Fujibayashi, K. Tamura, and N. Haruta, *J. Appl. Polym. Sci.* **54**, 2051 (1994).
- ¹⁸A. J. Meuler, J. D. Smith, K. K. Varanasi, J. M. Mabry, G. H. McKinley, and R. E. Cohen, *ACS Appl. Mater. Interfaces* **2**(11), 3100 (2010).
- ¹⁹A. J. Meuler, G. H. McKinley, and R. E. Cohen, *ACS Nano* **4**, 7048 (2010).
- ²⁰S. Jung, M. Dorrestijn, D. Raps, S. Das, C. M. Megaridis, and D. Poulikakos, *Langmuir* **27**, 3059 (2011).
- ²¹M. Nosonovsky and V. Hejazi, *ACS Nano* **6**, 8488 (2012).
- ²²J. A. van Meel, R. P. Sear, and D. Frenkel, *Phys. Rev. Lett.* **105**, 205501 (2010).
- ²³G. I. Tóth, G. Tegze, T. Pusztai, and L. Gránágy, *Phys. Rev. Lett.* **108**, 025502 (2012).
- ²⁴J. Chen, J. Liu, M. He, K. Li, D. Cui, Q. Zhang, X. Zeng, Y. Zhang, J. Wang, and Y. Song, *Appl. Phys. Lett.* **101**, 111603 (2012).
- ²⁵F. Leroy and F. Müller-Plathe, *Langmuir* **27**, 637 (2011).
- ²⁶F. Leroy and F. Müller-Plathe, *J. Chem. Theory Comput.* **8**, 3724 (2012).
- ²⁷V. Molinero and E. B. Moore, *J. Phys. Chem. B* **113**, 4008 (2009).
- ²⁸T. Werder, J. H. Walther, R. L. Jaffe, T. Halicioglu, and P. Koumoutsakos, *J. Phys. Chem. B* **107**, 1345 (2003).
- ²⁹E. B. Moore, T. J. Allen, and V. Molinero, *J. Phys. Chem. C* **116**, 7507 (2012).
- ³⁰P. J. Steinhardt, D. R. Nelson, and M. Ronchetti, *Phys. Rev. B* **28**, 784 (1983).
- ³¹T. Li, D. Donadio, G. Russoc, and G. Gallicci, *Phys. Chem. Chem. Phys.* **13**, 19807 (2011).
- ³²S. Plimpton, *J. Comput. Phys.* **117**, 1 (1995).
- ³³N. H. Fletcher, *Sci. Prog. Oxf.* **54**, 227 (1966).
- ³⁴E. B. Moore, E. d. l. Llave, K. Welke, D. A. Scherlis, and V. Molinero, *Phys. Chem. Chem. Phys.* **12**, 4124 (2010).
- ³⁵M. Heni and H. Löwen, *Phys. Rev. Lett.* **85**, 3668 (2000).
- ³⁶W. Xu, Z. Sun, and L. An, *J. Chem. Phys.* **132**, 144506 (2010).
- ³⁷S. Auer and D. Frenkel, *Phys. Rev. Lett.* **91**, 015703 (2003).
- ³⁸T. Li, D. Donadio, L. M. Ghiringhelli, and G. Galli, *Nature Mater.* **8**, 726 (2009).
- ³⁹K. Li, S. Xu, W. Shi, M. He, H. Li, S. Li, X. Zhou, J. Wang, and Y. Song, *Langmuir* **28**, 10749 (2012).
- ⁴⁰K. K. Varanasi, T. Deng, J. D. Smith, M. Hsu, and N. Bhate, *Appl. Phys. Lett.* **97**, 234102 (2010).
- ⁴¹See supplementary material at <http://dx.doi.org/10.1063/1.4862257> for rough surface model, ice profile on smooth surfaces, snapshots of crystallization at different wetting states, density and energy profiles on rough surfaces, and tabulated summary of freezing temperature and work of adhesion.